Chromosome Res (2015) 23:211–223
DOI 10.1007/s10577-014-9461-5

Intragenomic distribution of *RTE* retroelements suggests intrachromosomal movement

Eugenia E. Montiel · Francisco J. Ruiz-Ruano · Josefa Cabrero · Juan Alberto Marchal · Antonio Sánchez · Francisco Perfectti · María Dolores López-León · Juan Pedro M. Camacho

Received: 20 September 2014 / Revised: 25 November 2014 / Accepted: 18 December 2014 / Published online: 21 January 2015

Abstract Much is known about the abundance of transposable elements (TEs) in eukaryotic genomes, but much is still unknown on their behaviour within cells. We employ here a combination of cytological, molecular and genomic approaches providing information on the intragenomic distribution and behaviour of non-long terminal repeat (LTR) retrotransposon-like elements (*RTE*). We microdissected every chromosome in a single first meiotic metaphase cell of the grasshopper *Eyprepocnemis plorans* and polymerase chain reaction (PCR) amplified a fragment of the *RTE* reverse transcriptase gene with specific primers. PCR products were cloned and 139 clones were sequenced. Analysis of molecular variance (AMOVA) showed significant intragenomic structure for these elements, with 4.6 % of molecular variance being found between chromosomes. A maximum likelihood tree built with the *RTE* sequences revealed the frequent presence of two or more elements showing very high similarity and being located on the same chromosome, thus suggesting intrachromosome movement. The 454 pyrosequencing of genomic DNA gave strong support to the microdissection results and provided evidence for the existence of 5′ truncated elements. Our results thus indicate a tendency of *RTE* elements to reinsert into the same chromosome from where they were transcribed, which could be achieved if retrotranscription and insertion takes place immediately after transcription.

Responsible Editor: Rachel O'Neill

Eugenia E. Montiel and Francisco J. Ruiz-Ruano contributed equally to this study.

Electronic supplementary material The online version of this article (doi:10.1007/s10577-014-9461-5) contains supplementary material, which is available to authorized users.

E. E. Montiel · F. J. Ruiz-Ruano · J. Cabrero · F. Perfectti · M. D. López-León · J. P. M. Camacho (✉)
Departamento de Genética, Facultad de Ciencias, Universidad de Granada, Granada 18071, Spain
e-mail: jpmcamac@ugr.es

E. E. Montiel
e-mail: emontiel@gmail.com

F. J. Ruiz-Ruano
e-mail: fjruizruano@gmail.com

J. Cabrero
e-mail: jcabrero@ugr.es

F. Perfectti
e-mail: fperfect@ugr.es

M. D. López-León
e-mail: mdlopez@ugr.es

J. A. Marchal · A. Sánchez
Departamento de Biología Experimental, Facultad de Ciencias Experimentales, Universidad de Jaén, Jaén, Spain

J. A. Marchal
e-mail: jamaor@ujaen.es

A. Sánchez
e-mail: abaca@ujaen.es

Keywords 454 sequencing · Intrachromosomal · Intragenomic · Microdissection · RTE · Transposable elements

Abbreviations

AMOVA	Analysis of molecular variance
dNTP	Deoxynucleoside triphosphate
LINE	Long interspersed nuclear element

LTR	Long terminal repeat
ORF	Open reading frame
PCR	Polymerase chain reaction
RTE	Non-LTR retrotransposon-like element
SINE	Short interspersed nuclear element
TE	Transposable element

Introduction

As evidenced by the genomes recently sequenced, eukaryote genomes contain huge amounts of transposable elements (TEs): 15 % of the *Drosophila melanogaster* genome (Vieira et al. 1999), 45 % of the human genome (Lander et al. 2001) and up to 80 % in some plant genomes (Charles et al. 2008; Tenaillon et al. 2011). TEs are usually classified as class I (retrotransposons), with an RNA intermediate, and class II (transposons) (Wicker et al. 2007). On the basis of the presence or absence of long terminal repeats (LTRs), retrotransposons are classified into LTR and non-LTR elements, respectively. The latter include short interspersed nuclear elements (*SINE*s) and long interspersed nuclear elements (*LINE*s) which are the most widespread TEs in eukaryotes (Vitte and Bennetzen 2006). Retrotransposon-like element (*RTE*) is a non-LTR retrotransposon that is very abundant in most eukaryotes. It is a kind of *LINE* showing an integration mechanism through target-primed reverse transcription which frequently generates 5′ truncated copies due to the integration of prematurely terminated reverse transcripts (Malik and Eickbush 1998). This implies the simultaneous reverse transcription and joining of the 5′ end of the first-strand complementary DNA (cDNA) with the genome thus starting integration (Zingler et al. 2005). Since reverse transcription and integration occur simultaneously, the logical consequence of reverse transcription interruption is the integration of 5′ truncated copies. It is known that non-LTR retrotransposons, including *LINE*-1 in humans, perform reverse transcription in the nucleus, but the ultimate cause for 5′ truncation remains mostly unknown (Zingler et al. 2005).

The intragenomic distribution of TEs could illuminate some obscure aspects of their behaviour. For this purpose, we assay here a combination of the microdissection of each chromosome in a single cell and subsequent polymerase chain reaction (PCR) amplification of part of the *RTE* sequence, with sequence comparisons between elements residing in different chromosomes. Chromosome microdissection was developed by Scalenghe et al. (1981) in polytene chromosomes of *Drosophila*, and shortly after, it was applied to human chromosomes (Bates et al. 1986). From then on, many different applications have emerged (Cannizzaro 1996; Zhou and Hu 2007). One of the main current uses of chromosome microdissection is for chromosome painting (Guan et al. 1994; Houben et al. 2001; Marchal et al. 2004; Teruel et al. 2009), but it has rarely been used for the analysis of specific DNA sequences from specific chromosomes (Cheng and Lin 2003; Lamb et al. 2005; Teruel et al. 2010), even though this latter approach may be very useful for a broad range of genomic studies. For instance, clinical genetics has taken particular advantage of microdissection, facilitating genetic disease analysis such as the identification of the affected genes in Prader-Willi syndrome (Buiting et al. 1990) or characterization of marker chromosomes in prenatal diagnosis (Mahjoubi et al. 2005).

Here, we perform the microdissection of all chromosomes in a single cell and amplify in them, by PCR, a fragment of the *RTE* retrotransposon, in order to analyse the intragenomic distribution of these elements in the grasshopper *Eyprepocnemis plorans*, a species with a gigantic genome (Ruiz-Ruano et al. 2011) that is rich in mobile elements such as *Gypsy* and *RTE* retrotransposons and *Mariner* transposons (Montiel et al. 2012). They are widely represented in euchromatic regions of all standard (A) chromosomes and, in a lesser extent, on B chromosomes (a kind of dispensable heterocromatic chromosomes) (Camacho 2005). We also performed 454 pyrosequencing of genomic DNA to test the reliability of the DNA sequences obtained through microdissection and PCR amplification. The coding nature of *RTE* provided us with useful tools to test the action of purifying selection during the evolutionary dynamics of these elements.

Materials and methods

Microdissection and PCR-cloning experiment

We microdissected all chromosomes (11 autosomal bivalents and X and B univalents) out of a previously photographed single spermatocyte at first meiotic metaphase (Fig. S1), from a B-carrying male captured in Torrox (Málaga, Spain). Chromosomes were stored into

separate 0.2-ml Eppendorf tubes with 1X Buffer Taq polymerase (MBL) and 2 mg/ml proteinase K (Sigma), to be subsequently denatured at 50 °C for 1 h and at 99 °C for 4 min. Chromosomes were named in order of decreasing area, excepting X and B univalents which were easily identified because of their differential heteropycnosis, size and univalency. Chromosome area was measured (in arbitrary units) using the ImageJ program, version 1.44p (http://imagej.nih.gov/ij). Measures were repeated three times to corroborate the results. PCR reactions were performed on each chromosome, to amplify the YLG motive of region 7 of the reverse transcriptase gene of the *RTE* element (see Xiong and Eickbush 1990), with the primers qPCR_RTEf (5′-AGA TTG GGA AAC GAG GCA CTG-3′) and RTE_IntR (5′-CAT CCA TAC AAG GCA ACA CTC-3′), which yielded a 218-bp fragment coding to the thumb region of the reverse transcriptase enzyme (Xiong and Eickbush 1990; Montiel et al. 2012). The reaction mix was composed of 2 mM MgCl2, 0.16 mM deoxynucleoside triphosphate (dNTP), 4 % DMSO, 0.4 μM of each primer and 1 U Taq polymerase (MBL). The reaction conditions consisted in an initial denaturation step at 95 °C for 5 min followed by 30 cycles of 20 s at 94 °C, 30 s at 55 °C and 45 s at 72 °C, and a final extension for 8 min at 72 °C. PCR products were visualized in a 1 % agarose gel, and the fragment obtained from each chromosome was extracted from the gel with the GenElute Kit (Sigma), cloned into TOPO TA vector (Invitrogen) and transformed into One Shot TOP10 cell (Invitrogen). The insert of 17–28 clones per chromosome was sequenced in both directions (Macrogen) using the standard M13 primers. DNA sequences (GenBank: JX244482-JX244770) were aligned with the program BioEdit (Hall 1999) using ClustalW (Thompson et al. 1994). Saturation tests, performed following the procedure described in (Xia et al. 2003), indicated the absence of saturation for *RTE* sequences. We built a phylogenetic tree by the maximum likelihood method with the online version of PHYML (Dereeper et al. 2008), using a GTR evolutionary model, employing the α-LTR method (Anisimova and Gascuel 2006) to calculate branch support, and using the SplitsTree4 program (Huson and Bryant 2006) to process the obtained tree. Arlequin 3.0 software (Excoffier et al. 2005) was used to test the genomic structure of these sequences using the analysis of molecular variance (AMOVA) test. For comparison, we performed this same analysis to the data by Kejnovsky et al. (2007) (accession numbers: DQ683758-969 and DQ922567-629).

Whole genome shotgun experiment

We performed a sampling of repetitive DNA sequences in the *E. plorans* genome by means of 454 Roche pyrosequencing of total genomic DNA from a male carrying two B chromosomes, captured at Torrox (Málaga, Spain) (1/8 plate). We deposited the raw reads in the NCBI's SRA database (accession number SRR1200829). After performing a quality trimming with Roche's 454 GS Assembler, and excluding those reads with a size lower than 200 nt, we cut the remaining reads into as many 200-nt-long fragments as possible. We applied the RepeatExplorer pipeline (Novák et al. 2013) in order to perform a clustering of the resulting fragments according to their identity, and performed a de novo assembly in each individual cluster to get a consensus sequence of the most frequent families of *RTE* elements present in the *E. plorans* genome. For each of the two clusters found by RepeatExplorer, we selected the largest contig. To identify the 5′ and 3′ ends and determine the depth along all the element sequence, we mapped all the reads to the selected contigs of each subfamily with the Roche's 454 GS Mapper, with defaults options, i.e. with a minimum overlap length of 40 bp and 90 % identity, and bearing in mind the dramatic decline in coverage at both ends, coinciding with the end of the microsatellite region in the 3′ end. The coding region with the longest open reading frame (ORF) was considered representative for each *RTE* subfamily (GenBank: KF881086 and KF881087). To analyse sequence conservation at protein level, we aligned the putative amino acid sequence of the *RTE* retroelements with that reported for *Bombyx mori* (accession number ADF18552).

We then extracted the reads, assigned them to one of the two clusters, and aligned them against the ORF region of the representative nucleotide sequence for each cluster with the RepeatMasker software (Smit et al. 2010). Using a custom Python script (https://github.com/fjruizruano/rmasker-processing), we processed the output to classify the reads as (i) completely aligned; (ii) partly aligned in the 5′ or 3′ regions, thus including the beginning or the end of *RTE* and (iii) partly aligned due to the presence of insertions or deletions. The aligned region of the reads belonging to the first two groups was analysed in the

appropriate reading frame and only those lacking indels and stop codons were considered as putatively functional (non-defective). The third type of reads was considered as defective.

Calculations of the number of *RTE* elements in the *E. plorans* genome were done at nucleotide level and then converted to elements considering element length. The proportion of the genome represented by *RTE* elements was calculated by dividing the *RTE* nucleotides between total nucleotides in the trimmed library. The number of *RTE* elements in the library was calculated by dividing the total number of *RTE* nucleotides between ORF length. The number of *RTE* elements in the 2B male was calculated by multiplying the number of elements in the library by the total number of base pairs in a 2B male (calculated as explained below) and dividing by the total number of nucleotides in the 454 library. The number of base pairs in a male genome from Torrox carrying two B chromosomes was estimated bearing in mind (i) that the *E. plorans C* value, the DNA content of the X chromosome and that of the B chromosome in this population are 1.78, 0.219 and 0.108 times the *C* value in *Locusta migratoria* (Ruiz-Ruano et al. 2011), (ii) that grasshopper males are X0, and (iii) that full genome sequence in *L. migratoria* is 6.3 Gb (Wang et al. 2014). Consequently, the number of base pairs in a 2B male is 2C−X+B×2=22.4 Gb. Divergence was calculated by RepeatMasker as the percentage of differences between each sequence read and the consensus sequence in the matched region. The divergence of each cluster was calculated as the mean divergence of read matched regions weighted for their length in base pairs.

Comparative analysis between microdissection and whole genome shotgun results

To validate the microdissection results, we repeated the same analyses previously applied to the 139 clones obtained through microdissection and PCR amplification but, in this case, with the same 178 nt DNA sequences obtained through 454 pyrosequencing. To analyse the similarity of the *RTE* sequences in these 139 clones and those obtained through 454 pyrosequencing, we aligned them, along with the primers used for PCR (see above), using the Geneious v4.8 software (Drummond et al. 2009). For this purpose, we extracted this 178 nt sequence for each *RTE* subfamily and used it as reference to map and select the 454 reads carrying the full 178-nt region for the *RTE-1_EP* or the *RTE-2_EP* subfamilies, using RepeatMasker and processing its output with the above mentioned Python script. We then performed an analysis of nucleotide polymorphism with DnaSP v.5 (Librado and Rozas 2009), for the following parameters: number of segregating sites (S), number of haplotypes (H), nucleotide diversity (π) and heterozygosity per site (Θ Watterson's estimator) (Watterson 1975). In addition, we tested for neutrality, positive and purifying selection, based on the comparison of the number of synonymous and non-synonymous substitutions per site by the codon-based tests of neutrality using the Nei-Gojobori method (Nei and Gojobori 1986) in MEGA 4.0 (Tamura et al. 2007). All positions containing gaps and missing data were eliminated from the dataset. Statistical analyses were performed with the software STATISTICA 6.0.

Results

Intragenomic distribution of *RTE* elements

We obtained RTE amplification from 11 out of the 13 microdissected chromosomes, the exceptions being the smallest autosome (S_{11}) and the B chromosome. The PCR amplification product from each chromosome was cloned and sequenced in both directions. After discarding primer regions, a total of 178 bp from the reverse transcriptase domain of the *RTE* element were obtained in 139 clones (Table 1), 79.1 % of which lacked indels and stop codons, suggesting that they were non-defective, and thus they could be putatively active. Defective sequences (i.e. those showing indels or stop codons) showed more than twice nucleotide diversity (π) as non-defective ones, and their heterozygosity per site (Θ) was about 50 % higher (Table 1).

We also compared synonymous and non-synonymous substitutions in non-defective *RTE* sequences to test whether selection was operating on them using codon-based tests of neutrality. It showed that the purifying selection was acting on these retroelements in most chromosomes except chromosome 2 where neutrality could not be rejected (Table 2), but this was probably due to the low number of sequences obtained from this chromosome (see Table 1).

Considering that our collection of *RTE* elements came from specific locations in the *E. plorans* genome (i.e. each of 10 chromosomes of the standard karyotype), we analysed the genetic structure of these 10

Table 1 Genetic variation found in the *RTE* sequences obtained through microdissection and PCR amplification

Chromosome	*N*	*H*	*s*	*S*	π	Θ
1	13	12	177	62	0.087	0.113
2	4	4	174	79	0.260	0.248
3	13	13	178	59	0.079	0.107
4	7	6	176	56	0.105	0.130
5	9	9	172	67	0.108	0.143
6	11	11	178	48	0.067	0.092
7	19	18	173	87	0.109	0.144
8	22	17	174	83	0.099	0.131
9	12	11	178	68	0.100	0.127
10	14	11	176	54	0.078	0.096
X	14	8	178	54	0.088	0.095
Non-defective	110	93	178	154	0.078	0.164
Defective	29	27	149	130	0.183	0.222
All	139	116	149	144	0.099	0.175

N number of sequences, *H* number of haplotypes, *s* number of sites, *S* number of segregating sites, π nucleotide diversity (per site) and Θ heterozygosity (per site) from number of mutations. Values have been calculated after exclusion of sites with gaps

population samples of DNA sequences by means of an AMOVA with all the 116 haplotypes obtained (including defective and non-defective elements and excluding gaps). The results indicated that most genetic variation was found within chromosomes (95.4 %), although there was also a significant variation among chromosomes (4.6 %) thus resulting in an F_{ST} value (0.046) being significantly higher than zero (Table 3).

With all *RTE* sequences, defective and non-defective, we built a tree (Fig. 1) which showed most branches composed of *RTE* elements coming from several different chromosomes. However, there were 13 branches containing 2–4 sequences from the same chromosome showing very high similarity. Only three of these branches involved defective elements whereas the remaining 10 involved non-defective elements. The chromosomes most frequently showing this pattern were the X chromosome (four branches, one of them with one defective and one non-defective elements); chromosome 10 (three branches, one of them involving defective elements); chromosome 8 (with two branches) and chromosomes 1, 4, 7 and 9 (with one branch each, the elements in chromosome 7 being defective). This pattern suggests a tendency of *RTE* to reinsert into the same chromosome from where it was transcribed. This could be achieved if transcribed RTE elements were retrotranscribed and reinserted immediately after transcription. One possible symptom of this behaviour could be 5′ truncations.

Table 2 Nei-Gojobori codon-based test of neutrality, positive selection and purifying selection performed to every group of sequences obtained from each microdissected chromosome

Chrom	dN (SE)	dS (SE)	dN/dS	Neutrality (dN = dS)		Positive selection (dN > dS)		Purifying selection (dN < dS)	
				Z	*P*	*Z*	*P*	*Z*	*P*
1	0.059 (0.011)	0.262 (0.067)	0.225	−4.138	<0.001	−3.899	1	4.053	<0.001
2	0.114 (0.035)	0.211 (0.087)	0.540	−1.162	0.248	−1.181	1	1.13	0.13
3	0.053 (0.01)	0.18 (0.045)	0.294	−3.377	0.001	−3.434	1	3.566	<0.001
4	0.021 (0.008)	0.108 (0.045)	0.194	−2.112	0.037	−2.17	1	2.05	0.021
5	0.041 (0.011)	0.148 (0.047)	0.277	−2.686	0.008	−2.71	1	2.781	0.003
6	0.038 (0.008)	0.131 (0.034)	0.290	−3.222	0.002	−3.252	1	3.296	0.001
7	0.085 (0.013)	0.262 (0.052)	0.324	−3.96	<0.001	−4.285	1	4.074	<0.001
8	0.033 (0.008)	0.105 (0.036)	0.314	−2.178	0.031	−2.195	1	2.243	0.013
9	0.068 (0.013)	0.255 (0.063)	0.267	−3.487	0.001	−3.69	1	3.63	<0.001
10	0.062 (0.013)	0.174 (0.055)	0.356	−2.402	0.018	−2.226	1	2.532	0.006
X	0.05 (0.012)	0.553 (0.159)	0.090	−5.067	<0.001	−5.079	1	5.265	<0.001

Chrom Chromosome, *dN* Number of non-synonymous substitutions per site, *dS* Number of synonymous substitutions per site, *SE* Standard error, *Z* *Z* statistics, *P* *P* value

Table 3 AMOVA with the 116 haplotypes found among the *RTE* sequences obtained through microdissection and PCR

Source of variation	*df*	Sum of squares	Variance components	Percentage of variation
Among chromosomes	10	142.97	0.41	4.20
Within chromosomes	128	1184.87	9.25	95.80
Total	138	1327.26	9.66	

F_{ST}=0.042

Significance tests (1023 permutations)

Vamong and F_{ST}: *P* (rand. value > obs. value) <0.00001

P value <0.00001±0.00001

5′ truncations in *RTE* elements

The 454 sequencing experiment performed on genomic DNA from a 2B male yielded 128,572 reads summing up to 80,996,774 nt (N50=733 nt) after quality trimming and 117,694 reads summing up to 79,842,732 nt (N50=735 nt) after length trimming. Since the *E. plorans* genome consists of 11.21 Gb in the Torrox population (Ruiz-Ruano et al. 2011) (see "Materials and methods" section), the reads obtained implied a 0.0071× coverage per nucleotide. Although this is insignificant for single-copy genes, it resulted as very informative for repetitive DNA analysis where coverage is multiplied by the number of paralogous copies in the genome. Among the repetitive sequences assembled by RepeatExplorer, we found two subfamilies annotated as *RTE* with 62.1 % pairwise identity. One of them (*RTE-1_EP*) represented 3.74 % of the sequenced nucleotides, and the other (*RTE-2_EP*), constituted 1.18 % of them. As a whole, the *RTE* retrotransposon was the most abundant repetitive element, representing 4.92 % of all sequenced nucleotides. In close resemblance to the RTE elements in other insect orders (Tay et al. 2010), we found *RTE-1_EP* and *RTE-2_EP* elements in *E. plorans* being 3315 and 3360 pb long, respectively. In both subfamilies we found a 5′-UTR with 315 (*RTE-1_EP*) and 344 (*RTE-2_EP*) nt, a single ORF of 2961 and 2970 bp (987 and 990 amino acids), respectively, with a TGA stop codon, and a 3′-UTR of 39 and 46 nt, respectively, with $(CCA)_{11}$ and $(A)_{42}$ terminal microsatellite regions in *RTE-1_EP* and *RTE-2_EP*, respectively. The alignment with the amino acidic sequence in *B. mori* indicated the presence of the apurinic endonuclease domain (pfam03372) followed by the reverse transcriptase domain (pfam00078). We found no target site duplications because read size was smaller than element size and reads aligned in the ends of the elements could come from insertions in different sites. The existence of these conserved regions in the RTE sequence genome and the high abundance of this element in the *E. plorans* genome suggest a recent or current functionality of both RTE subfamilies.

The analysis of the coded amino acid sequence indicated that at least 92.76 % of the *RTE-1_EP* and 89.88 % of the *RTE-2_EP RTE* reads showed stop codons thus being defective (Table 4). In both subfamilies, defective elements showed higher divergence in respect to the consensus sequence used as reference (Novák et al. 2013), and *RTE-1_EP* elements showed higher divergence than *RTE-2_EP* ones (Table 4 and Fig. 2).

In non-LTR retrotransposons, the existence of 5′ truncated copies is indicative of the integration of prematurely terminated reverse transcripts initiating at the 3′ end of the RNA (Luan et al. 1993). If this behaviour were frequent for *RTE* elements in the *E. plorans* genome, we would expect lower coverage in 5′ regions, compared to 3′ ones. To test this hypothesis, we mapped the 454 reads from the genomic library on the assembled *RTE-1_EP* and *RTE-2_EP* elements in order to estimate coverage per nucleotide position (Fig. 3). In both cases, we observed lower coverage in the 5′ end in respect to that in the 3′ end (sixfold bias for *RTE-1_EP* and threefold bias for *RTE-2_EP*). This result is consistent with the existence of 5′ truncated copies for *RTE* elements in the *E. plorans* genome.

We finally searched for insertion of other elements within *RTE* elements, as evidenced by the presence of two consecutive *RTE* segments, within a same read,

Fig. 1 Phylogenetic tree of *RTE* element fragments amplified ▶ from every chromosome in *E. plorans*. Chromosomes are differentiated by *colour* as indicated in the figure. Defective copies are marked with a *cross mark*. Note the clustering of very similar *RTE* elements coming from the same chromosome (*arrows*)

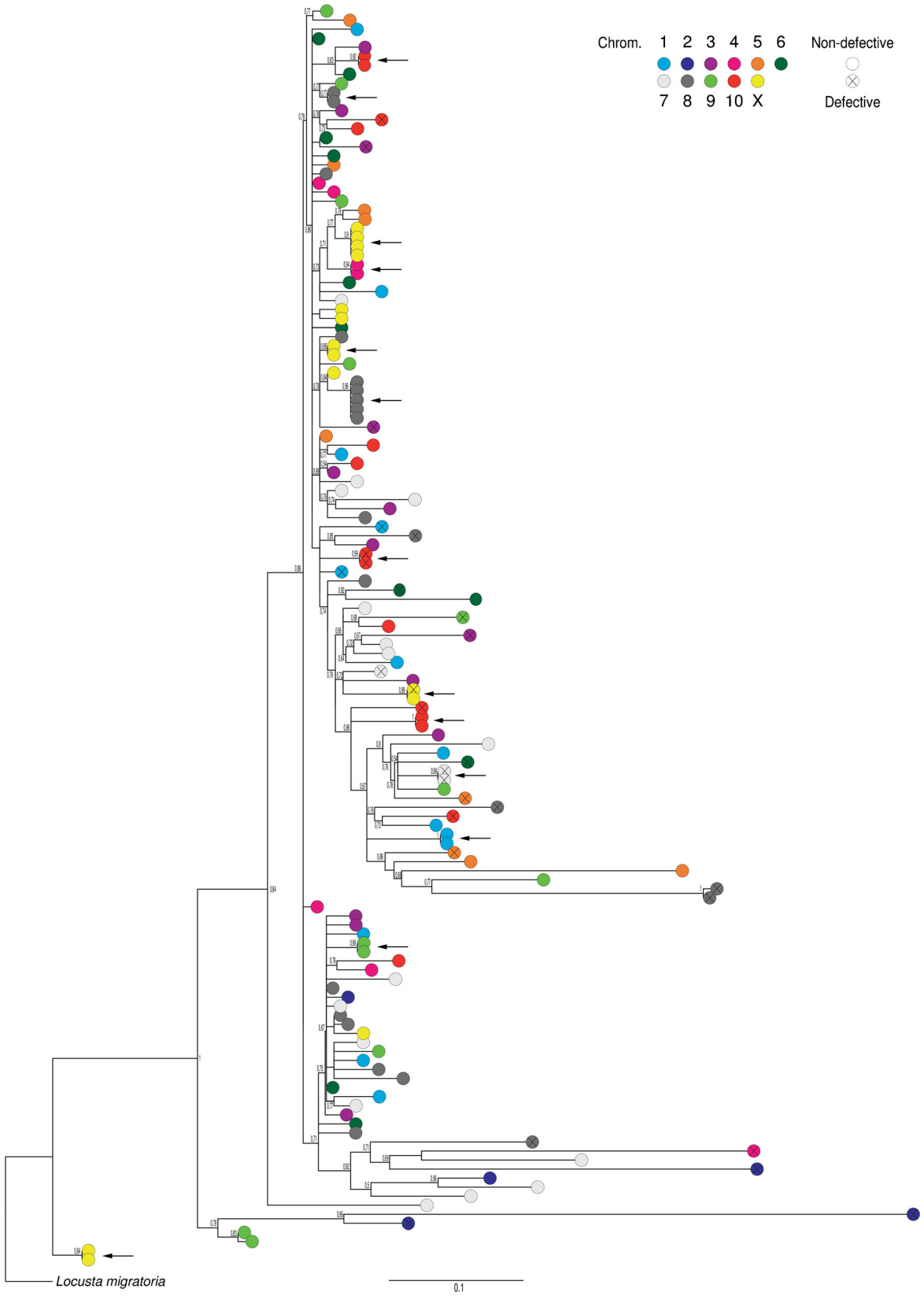
Chrom. 1 2 3 4 5 6
7 8 9 10 X
Non-defective
Defective
Locusta migratoria
0.1

Table 4 1Number of defective and non-defective *RTE* elements found in the *E. plorans* genome, estimated from the 454 reads, for the *RTE-1_EP* and *RTE-2_EP* subfamilies

RTE	Item	Non-defective	Defective	Total
RTE-1_EP	Total *RTE* nucleotides	216,041	2,766,699	2,982,740
	%	7.24	92.76	100
	% of the genome	0.27	3.47	3.74
	No. *RTE* elements in the library	73	934	1007
	No. *RTE* elements in the 2B male	20,470	262,142	282,611
	Divergence	4.2	6.9	6.7
RTE-2_EP	Total *RTE* nucleotides	95,238	845,965	941,203
	%	10.12	89.88	100
	% of the genome	0.12	1.06	1.18
	No. *RTE* elements in the library	32	285	317
	No. *RTE* elements in the 2B male	8996	79,911	88,908
	Divergence	3.2	4.5	4.4

interrupted by a short non-*RTE* sequence. We found a total of 195 *RTE-1_EP* interrupted elements and 46 *RTE-2_EP* interrupted elements. Annotation of the sequences inserted into *RTE* elements showed that most of them were *SINE*s (Table 5).

Comparison of PCR-cloning and 454 sequencing results

The alignment of the 139 sequences obtained from microdissected chromosomes with the *RTE-1_EP* and *RTE-2_EP* consensus sequences indicated that all of them showed higher identity with the *RTE-1_EP* subfamily. In fact, *RTE-2_EP* elements could not have been amplified with the employed primers because of sequence differences (Fig. S2).

A comparison of the proportion of defective and non-defective elements inferred from the 178-bp fragments amplified by PCR from individual chromosomes, with the same figures inferred from this same region in the *RTE-1_EP* elements obtained from the 454 reads revealed some differences. Logically, this shorter window yielded lower amounts of non-functional elements than

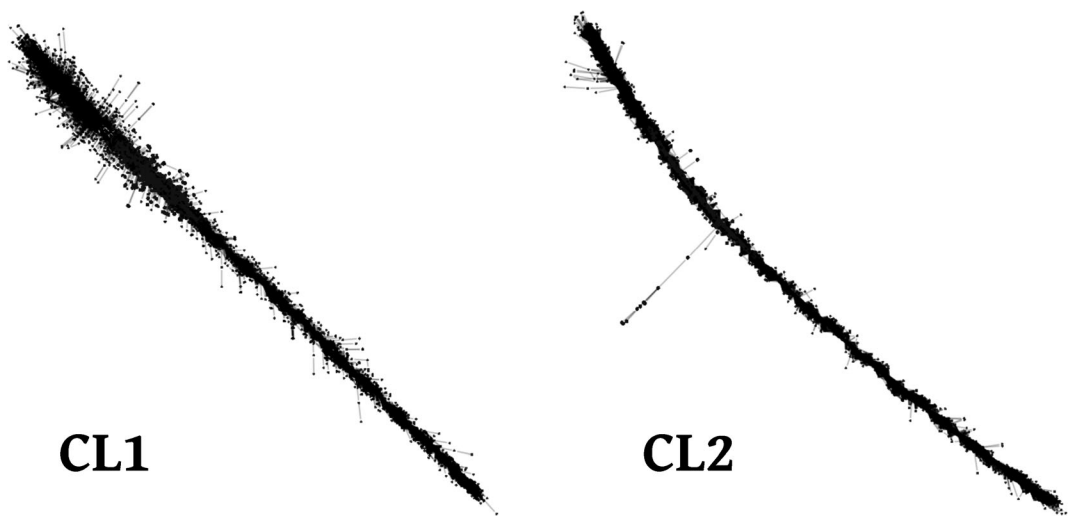

Fig. 2 Graph layouts of the two clusters of *RTE* elements (subfamilies) obtained, after 454 sequencing, yielded by the RepeatMasker software. Note the higher variation in the *RTE-1_EP* subfamily

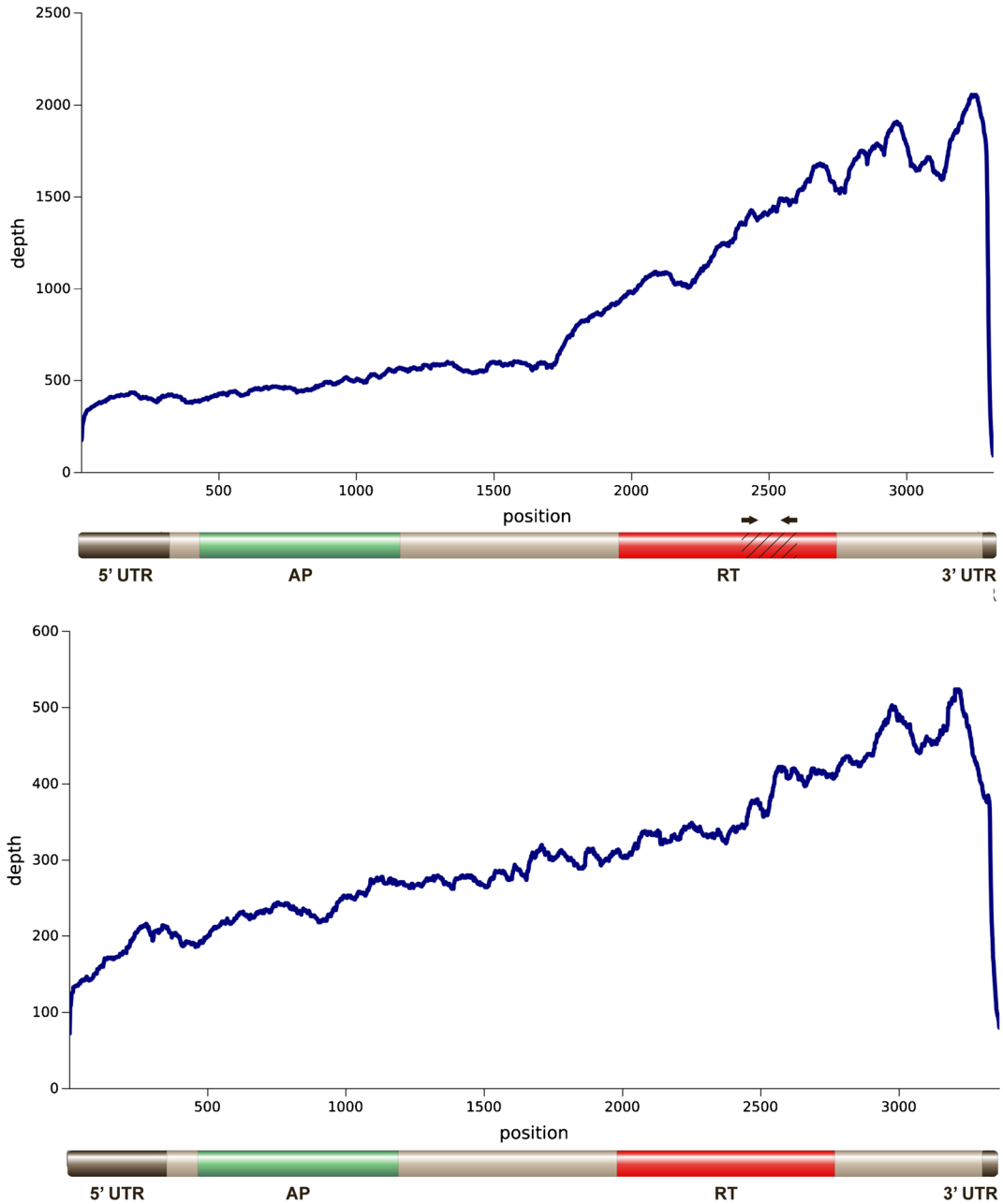

Fig. 3 Coverage per nucleotidic position for *RTE-1_EP* (*upper panel*) and *RTE-2_EP* (*lower panel*) elements. Diagrams show a representation of *RTE-1_EP* and *RTE-2_EP* elements indicating the position of 5′UTR and 3′UTR (*dark grey boxes*), apurinic endonuclease domain (*green box*) and reverse transcriptase domain (*red box*), as well as the primer-binding position (*arrows*) and the region amplified by PCR (*striped area*)

the analysis across the full RTE sequence shown in Table 4. However, the proportion of non-defective elements (40.73 %, see counts in Table S1) was still lower than the 79 % observed in the PCR-amplified fragments. This difference could be due to PCR bias towards non-defective sequences, since many of the defective ones could carry sequence changes impeding primer anchoring.

The analysis of nucleotide diversity for the 178-bp fragment (Table S2), performed in the 454 reads showed

Table 5 Annotation of DNA sequences interrupting *RTE* elements found in the 454 reads

Item	*RTE-1_EP*	*RTE-2_EP*
SINE - HASE1	4	0
SINE - HASE1 - Afrosine1b	4	0
SINE - MIRc	16	3
DNA - Chompy-7 Croc	45	0
SINE - 2b1 - SGRP1	6	3
SINE - LM1	62	17
No match	58	19

remarkably similar values to those observed in the PCR-cloning experiment, especially for non-defective elements (0.081 versus 0.078) (compare Tables 1 and S2). However, in defective elements, nucleotide diversity deduced from 454 pyrosequencing (0.28) was higher than that observed in the PCR-cloning experiment (0.18), presumably due to the PCR bias.

Finally, the Nei-Gojobori codon-based test showed that the 178 bp in the two types of RTE elements (i.e. *RTE-1_EP* and *RTE-2_EP*) found in the 454 reads, were subjected to purifying selection (Table S3), in consistency with the observations in the PCR-cloning experiment. Remarkably, this was apparent in both defective and non-defective *RTE* elements, although the dN/dS ratio was higher in defective elements in both *RTE-1_EP* and *RTE-2_EP* subfamilies (see Table S3).

Discussion

Our analysis of part of the reverse transcriptase gene from *RTE* elements in the grasshopper *E. plorans*, by means of microdissection of individual chromosomes, PCR amplification, cloning and sequencing, has provided valuable information on their intragenomic structure. Most of the analysed DNA sequences (79 %) lacked stop codons or indels, and we considered them as non-defective. But the 178 bp analysed only represent 5.3 % of total DNA sequence in full-length elements and they were analysed through PCR, which clearly yielded a bias towards non-defective elements. In fact, our 454 pyrosequencing analysis of genomic DNA showed less than 10 % of non-defective elements. Therefore, most *RTE* elements in the *E. plorans* genome appear to be defective thus forming a part of the presumable huge amounts of repetitive DNA in the gigantic genome of *E. plorans*, containing more than 10^{10} bp (Ruiz-Ruano et al. 2011).

Although the diversity of retro- and transposon families has been widely analysed (Bartolomé et al. 2002; Gomulski et al. 2004; Hollister and Gaut 2007), only a few studies have connected diversity with chromosome location. Good examples of this kind of work are found in (Hood et al. 2005), where they analyse the genetic structure of *Copia* and *Helitron* families in electrophoretically separated chromosomes from *Microbotryum violaceum*. Likewise, Kejnovsky et al. (2007) analysed diversity for *Retand*, a *Gyspy*-like retrotransposon, in microdissected sex chromosomes and autosomes in *Silene latifolia*. Our present study, however, is the first trying to ascertain the intragenomic distribution of *RTE* retroelements including all standard chromosomes and also B chromosomes.

The degree of nucleotide diversity in the *RTE* elements found in *E. plorans* (about 0.08 in non-defective elements and 0.28 for defective elements) is larger than that observed for other DNA sequences in *E. plorans*, such as, for instance, the ITS-1 region in the ribosomal DNA (π=0.014) (Teruel et al. 2014), a fact being expected for elements using an RNA molecule as transposition intermediate and not submitted to concerted evolution. These diversity values are one order of magnitude larger than those reported for active copies of LTR and non-LTR elements in *D. melanogaster* (Sánchez-Gracia et al. 2005), and also higher than those reported for *TOPI* elements in *Anopheles gambiae* (π=0.051) (Subramanian et al. 2008).

Such high nucleotide diversity would appear to be difficult to reconcile with the action of purifying selection for a functional reverse transcriptase sequence of *RTE* elements. However, the separate analysis of defective and non-defective elements (see Table S3) indicates that selection has relaxed in defective elements since their dN/dS ratio was higher than that in non-defective ones. It has been shown that both LTR and non-LTR retrotransposons can show two different evolutionary patterns: a pseudogene-like mode through neutral evolution after insertion and nonfunctionalization, and a gene-like mode being characterized by the action of purifying selection to maintain element functionality (Bergman and Bensasson 2007). Retrotransposons following a pseudogene-like evolutionary pattern thus become genomic relics evolving under the absence of selective constraints. We have not found this pseudogene-like pattern in *RTE*, at least with the limited

information provided by the 178-bp sequence analysed, since the codon-based tests showed evidence for purifying selection in both non-defective and defective elements. Interestingly, defective *RTE* elements appear to conserve the bias for synonymous substitutions promoted by purifying selection, a signal which could not be erased even after long periods of neutral evolution.

The observed intragenomic structure of *RTE* elements in the *E. plorans* genome, and their tendency to show a certain degree of intrachomosomal similarity, could be the result of *RTE* tendency to reinsert into the same chromosome from where it was transcribed, which could be more likely if the time between transcription and reverse transcription is short and the transcript scarcely moves before reinsertion (i.e., space and time are both small and short, respectively). This is feasible since chromosomes tend to occupy certain territories in the interphase nucleus (Cremer and Cremer 2001), and is consistent with the fact that, in non-LTR retrotransposons, including *LINE*-1 in humans (Zingler et al. 2005), reverse transcription occurs in the nucleus, and the integration of prematurely terminated reverse transcripts generates 5′ truncated copies in the *R2* retrotransposon (Luan et al. 1993). We have consistently found evidence for 5′ truncated copies for *RTE* elements in *E. plorans*. It is thus conceivable that these features of *RTE* behaviour can facilitate preferential intrachromosome retrotransposition, the net result being the existence of some genomic structure for *RTE* chromosome location. Interestingly, it has recently been shown that CoT-1 RNA including 5′ truncated LINE-1 elements, is abundant and stably associated with the chromosome from which it was transcribed, with the likely role of promoting open chromatin packaging (Hall et al. 2014). Our present results suggest that some of these LINE transcripts can be retrotranscribed and reinserted into the same chromosome while they are in its territory.

Alternatively, the intrachromosomal similarity observed for *RTE* elements in the *E. plorans* genome could be the result of homogenizing gene conversion. Kejnovsky et al. (2007) found intrachromosomal similarity for the *Retand* LTR retrotransposon in the plant *S. latifolia*, with elements residing in the X and Y chromosomes showing higher intrachromosomal similarity. We performed the AMOVA test to these authors' data which revealed very significant molecular structure for these retrotransposons, with 30 % of molecular variance among chromosomes (Table S4). These authors ruled out the possibility of preferential intrachromosome retrotransposition because, in LTR retroelements, reverse transcription occurs in the cytoplasm thus making it unlikely reinserting into the same chromosome. Alternatively, they explained this case by active gene conversion homogenizing intrachromosomal copies. We believe that this explanation is not applicable to *RTE* in *E. plorans* since, in sexually reproducing organisms, the homogenization processes are accelerated by meiotic recombination, and the gene conversion hypothesis would not be consistent with the fact that the X chromosome shows meiotic recombination only in females (males are X0) but that it showed the highest number of cases of intrachromosomal similarity.

A second alternative explanation for these results is random resampling of a single element from the same chromosome. This would be expected to occur more likely in small chromosomes. However, the fact that the chromosome where most cases of very similar *RTE* elements were found was the X chromosome, which is one of the largest chromosomes in the *E. plorans* genome, runs against this possibility.

The results of the 454 pyrosequencing showed that the *RTE* elements amplified on microdissected chromosomes belong to the most abundant *RTE* subfamily (*RTE-1_EP*) in the *E. plorans* genome. Perhaps the fact that *RTE* is one of the most abundant repetitive elements in the genome of *E. plorans* (Ruiz-Ruano et al., unpublished) facilitated very much the success of our present microdissection experiments. In any case, it should be worth trying in other species.

Finally, the apparent absence of *RTE* elements in B chromosomes is not consistent with the prediction that B chromosomes are havens for mobile elements (Camacho et al. 2000). This could be due to the fact that *RTE* elements are preferentially located at euchromatic regions in *E. plorans* (Montiel et al. 2012) and B chromosomes in this species are mostly heterochromatic. In spite of this, a small amount of *RTE* elements are still apparent in the B chromosomes of this species (Montiel et al. 2012). This could also be due to the PCR bias if most *RTE* elements in the B chromosome are defective. Another conceivable explanation for the absence of *RTE* elements in the B chromosomes comes from the fact that Bs probably derived from the smallest

autosome (S_{11}) and, as our present results have shown, *RTE* elements appear to be scarce in the latter chromosome. This would be consistent with our recent finding that the ITS regions of the ribosomal DNA contained in the B chromosome are more similar to those in the S_{11} than to those in other A chromosomes (Teruel et al. 2014).

Conclusions

The analysis of intragenomic distribution of *RTE* elements, by means of PCR amplification on DNA obtained from individually microdissected chromosomes, indicated a tendency of *RTE* elements to reinsert into the same chromosome from which they were transcribed. The analysis of 454 pyrosequenced genomic DNA supported these results and provided evidence for abundance of 5′ truncations in the *RTE* elements occurring through premature termination of reverse transcription. All these results, together, suggest that, in some cases, *RTE* reinsertion takes place immediately after transcription, while the transcript is yet located in the territory of the same chromosome.

Acknowledgments We thank Karl R. Meunier for the English review. This study was supported by the Plan Andaluz de Investigación (P10-CVI-6649), and was partially performed by FEDER funds.

References

Anisimova M, Gascuel O (2006) Approximate likelihood-ratio test for branches: a fast, accurate, and powerful alternative. Syst Biol 55:539–552

Bartolomé C, Maside X, Charlesworth B (2002) On the abundance and distribution of transposable elements in the genome of *Drosophila melanogaster*. Mol Biol Evol 19:926–937

Bates GP, Wainwright BJ, Williamson R, Brown SD (1986) Microdissection of and microcloning from the short arm of human chromosome 2. Mol Cell Biol 6:3826–3830

Bergman CM, Bensasson D (2007) Recent LTR retrotransposon insertion contrasts with waves of non-LTR insertion since speciation in *Drosophila melanogaster*. Proc Nat Acad Sci USA 104:11340–11345

Buiting K, Neumann M, Lüdecke HJ, Senger G, Claussen U, Antich J, Passarge E, Horsthemke B (1990) Microdissection of the Prader-Willi syndrome chromosome region and identification of potential gene sequences. Genomics 6:521–527

Camacho JPM (2005) B Chromosomes. In *The Evolution of the Genome*. Edited by Gregory T R. San Diego, 223–286

Camacho JPM, Sharbel TF, Beukeboom LW (2000) B-chromosome evolution. Philos Trans R Soc Lond B 355: 163–178

Cannizzaro LA (1996) Chromosome microdissection: a brief overview. Cytogenet Cell Genet 74:157–160

Charles M, Belcram H, Just J, Huneau C, Viollet A, Couloux A, Segurens B, Carter M, Huteau V, Coriton O, Appels R, Samain S, Chalhoub B (2008) Dynamics and differential proliferation of transposable elements during the evolution of the B and A genomes of wheat. Genetics 180:1071–1086

Cheng YM, Lin BY (2003) Cloning and characterization of maize B chromosome sequences derived from microdissection. Genetics 164:299–310

Cremer T, Cremer C (2001) Chromosome territories, nuclear architecture and gene regulation in mammalian cells. Nat Rev Genet 2:292–301

Dereeper A, Guignon V, Blanc G, Audic S, Buffet S, Chevenet F, Dufayard JF, Guindon S, Lefort V, Lescot M, et al. (2008) Phylogeny.fr: robust phylogenetic analysis for the non-specialist. Nucleic Acids Res 36(Web Server issue):W465-W469

Drummond AJ, Ashton B, Cheung M, Heled J, Kearse M, Moir R, Stones-Havas S, Thierer T, Wilson A (2009) Geneious v4.6. http://www.geneious.com/

Excoffier L, Laval G, Schneider S (2005) Arlequin (version 3.0): an integrated software package for population genetics data analysis. Evol Bioinforma Online 1:47–50

Gomulski LM, Torti C, Murelli V, Bonizzoni M, Gasperi G, Malacrida AR (2004) Medfly transposable elements: diversity, evolution, genomic impact and possible applications. Insect Biochem Mol 34:139–148

Guan XY, Meltzer PS, Trent JM (1994) Rapid generation of whole chromosome painting probes (WCPs) by chromosome microdissection. Genomics 22:101–107

Hall TA (1999) BioEdit: a user-friendly biological sequence alignment editor and analysis program for Windows 95/98/NT. Nucleic Acids Symp Ser 41:95–98

Hall LL, Carone DW, Gomez AV, Kolpa HJ, Byron M, Mehta N, Fackelmayer FO, Lawrence JB (2014) Stable CoT-1 repeat RNA is abundant and is associated with euchromatic interphase chromosomes. Cell 156:907–919

Hollister JD, Gaut BS (2007) Population and evolutionary dynamics of Helitron transposable elements in *Arabidopsis thaliana*. Mol Biol Evol 24:2515–2524

Hood ME, Katawczik M, Giraud T (2005) Repeat-induced point mutation and the population structure of transposable elements in *Microbotryum violaceum*. Genetics 170:1081–1089

Houben A, Field BL, Saunders VA (2001) Microdissection and chromosome painting of plant B chromosomes. Methods Cell Sci 23:115–124

Huson DH, Bryant D (2006) Application of phylogenetic networks in evolutionary studies. Mol Biol Evol 23:254–267

Kejnovsky E, Hobza R, Kubat Z, Widmer A, Marais GAB, Vyskot B (2007) High intrachromosomal similarity of retrotransposon long terminal repeats: evidence for homogenization by gene conversion on plant sex chromosomes? Gene 390:92–97

Lamb JC, Kato A, Birchler JA (2005) Sequences associated with A chromosome centromeres are present throughout the maize B chromosome. Chromosoma 113:337–349

Lander ES, Linton LM, Birren B et al (2001) Initial sequencing and analysis of the human genome. Nature 409:860–921

Librado P, Rozas J (2009) DnaSP v5: a software for comprehensive analysis of DNA polymorphism data. Bioinformatics 25: 1451–1452

Luan DD, Korman MH, Jakubczak JL, Eickbush TH (1993) Reverse transcription of R2Bm RNA is primed by a nick at the chromosomal target site: a mechanism for non-LTR retrotransposition. Cell 72:595–605

Mahjoubi F, Peters GB, Malafiej P, Shalhoub C, Turner A, Daniel A, Hill RJ (2005) An analphoid marker chromosome inv dup(15)(q26.1qter), detected during prenatal diagnosis and characterized via chromosome microdissection. Cytogenet Genome Res 109:485–490

Malik HS, Eickbush TH (1998) The RTE class of non-LTR retrotransposons is widely distributed in animals and is the origin of many SINE elements. Mol Biol Evol 15:1123–1134

Marchal JA, Acosta MJ, Bullejos M, Guardia RD, Sánchez A (2004) A repeat DNA sequence from the Y chromosome in species of the genus *Microtus*. Chromosome Res 12:757–765

Montiel EE, Cabrero J, Camacho JPM, López-León MD (2012) Gyspy, RTE and Mariner transposable elements populate *Eyprepocnemis plorans* genome. Genetica 140:365–374

Nei M, Gojobori T (1986) Simple methods for estimating the numbers of synonymous and nonsynonymous nucleotide substitutions. Mol Biol Evol 3:418–426

Novák P, Neumann P, Pech J, Steinhaisl J, Macas J (2013) RepeatExplorer: a Galaxy-based web server for genome-wide characterization of eukaryotic repetitive elements from next-generation sequence reads. Bioinformatics 29:792–793

Ruiz-Ruano FJ, Ruiz-Estévez M, Rodríguez-Pérez J, López-Pino JL, Cabrero J, Camacho JPM (2011) DNA Amount of X and B Chromosomes in the Grasshoppers *Eyprepocnemis plorans* and *Locusta migratoria*. Cytogenet Genome Res 134:120–126

Sánchez-Gracia A, Maside X, Charlesworth B (2005) High rate of horizontal transfer of transposable elements in Drosophila. Trends Genet 21:200–20328

Scalenghe F, Turco E, Edstrom JE, Pirrotta V, Melli M (1981) Microdissection and cloning of DNA from a specific region of *Drosophila melanogaster* polytene chromosomes. Chromosoma 82:205–216

Smit AFA, Hubley R, Green P (2010) RepeatMasker Open-3.0. 1996–2010 <http://www.repeatmasker.org>

Subramanian RA, Akala OO, Adejinmi JO, O'Brochta DA (2008) *Topi*, an IS630/Tc1/mariner-type transposable element in the African malaria mosquito, Anopheles gambiae. Gene 423:63–71

Tamura K, Dudley J, Masatoshi N, Kumar S (2007) MEGA4: molecular evolutionary genetics analysis (MEGA) software version 4.0. Mol Biol Evol 24:1596–1599

Tay WT, Behere GT, Batterham P, Heckel DG (2010) Generation of microsatellite repeat families by *RTE* retrotransposons in lepidopteran genomes. BMC Evol Biol 10:144

Tenaillon MI, Hufford MB, Gaut BS, Ross-Ibarra J (2011) Genome size and transposable element content as determined by high-throughput sequencing in maize and *Zea luxurians*. Genome Biol Evol 3:219–229

Teruel M, Cabrero J, Perfectti F, Acosta MJ, Sánchez A, Camacho JPM (2009) Microdissection and chromosome painting of X and B chromosomes in the grasshopper *Eyprepocnemis plorans*. Cytogenet Genome Res 125:286–291

Teruel M, Cabrero J, Perfectti F, Camacho JPM (2010) B chromosome ancestry revealed by histone genes in the migratory locust. Chromosoma 119:217–225

Teruel M, Ruíz-Ruano FJ, Marchal JA, Sánchez A, Cabrero J, Camacho JPM, Perfectti F (2014) Disparate molecular evolution of two types of repetitive DNA in the genome of the grasshopper *Eyprepocnemis plorans*. Heredity 112:531–542

Thompson JD, Higgins DG, Gibson TJ (1994) CLUSTAL W improving the sensitivity of progressive multiple sequence alignment through sequence weighting, position-specific gap penalties and weight matrix choice. Nucleic Acids Res 22:4673–4680

Vieira C, Lepetit D, Dumont S, Biemont C (1999) Wake up of transposable elements following *Drosophila simulans* worldwide colonization. Mol Biol Evol 16:1251–1255

Vitte C, Bennetzen JL (2006) Analysis of retrotransposon structural diversity uncovers properties and propensities in angiosperm genome evolution. Proc Natl Acad Sci U S A 2006(103):17638–17643

Wang X, Fang X, Yang P, Jiang X, Jiang F, Zhao D, Li B, Cui F, Wei J, Ma C, Wang Y, He J, Luo Y, Wang Z, Guo X, Guo W, Wang X, Zhang Y, Yang M, Hao S, Chen B, Ma Z, Yu D, Xiong Z, Zhu Y, Fan D, Han L, Wang B, Chen Y, Wang J et al (2014) The locust genome provides insight into swarm formation and long-distance flight. Nat Commun 5:2957

Watterson GA (1975) On the number of segregating sites in genetical models without recombination. Theor Popul Biol 7:256–276

Wicker T, Sabot F, Hua-Van A, Bennetzen JL, Capy P, Chalhoub B, Flavell A, Leroy P, Morgante M, Panaud O, Paux E, SanMiguel P, Schulman AH (2007) A unified classification system for eukaryotic transposable elements. Nat Rev Genet 8:973–982

Xia X, Xie Z, Salemi M, Chen L, Wang Y (2003) An index of substitution saturation and its application. Mol Phylogenet Evol 26:1–7

Xiong Y, Eickbush TH (1990) Origin and evolution of retroelements based upon their reverse transcriptase sequences. EMBO J 9:3353–3362

Zhou RN, Hu ZM (2007) The development of chromosome microdissection and microcloning technique and its applications in genomic research. Curr Genomics 8:67–72

Zingler N, Willhoeft U, Brose HP, Schoder V, Jahns T, Hanschmann KM, Morrish TA, Löwer J, Schumann GG (2005) Analysis of 5′ junctions of human LINE-1 and Alu retrotransposons suggests an alternative model for 5′-end attachment requiring microhomology-mediated end-joining. Genome Res 15:780–789

Supporting Tables

Table S1 Number (N) of defective and non-defective *RTE* elements inferred from the same 178 bp region analyzed in the PCR-cloning experiment but, in this case, analyzed through 454 sequencing of genomic DNA

	Non-defective		Defective	
Item	N	%	N	%
RTE-1_EP	433	40.73	630	59.27
RTE-2_EP	152	51.53	143	48.47

Table S2 Genetic variation found in the 178 bp region in the 454 reads

Item	Type	N	H	s	S	π	Θ
RTE-1_EP	Non-defective	433	359	180	175	0.081	0.148
	Defective	630	591	398	268	0.282	0.262
RTE-2_EP	Non-defective	152	133	178	159	0.063	0.160
	Defective	143	137	228	202	0.191	0.245

N: number of sequences, H: number of haplotypes, s: number of sites, S: number of segregating sites, π: nucleotide diversity (per site) and Θ: heterozygosity (per site) from number of mutations

Table S3 Nei-Gojobori codon-based test of neutrality, positive selection and purifying, applied to the 178 bp region of the RTE elements in the reads obtained by 454 sequencing of genomic DNA

				Neutrality ($d_N=d_S$)		Positive selection ($d_N>d_S$)		Purifying selection ($d_N<d_S$)	
Subfamily	dN (SE)	dS (SE)	dN/dS	Z	P	Z	P	Z	P
*RTE-1_EP*_ndef	0.050 (0.005)	0.205 (0.033)	0.244	-3.63	<0.001	-3.72	1	3.68	<0.001
*RTE-1_EP*_def	0.094(0.008)	0.195 (0.034)	0.482	-2954	0.004	-3.04	1	2.89	0.002
*RTE-2_EP*_ndef	0.046 (0.006)	0.127 (0.024)	0.362	-3.45	0.001	-3.31	1	3.74	<0.001
*RTE-2_EP*_def	0.078 (0.007)	0.165 (0.019)	0.473	-4.02	<0.001	-4.15	1	4.01	<0.001

dN: Number of non-synonymous substitutions per site, dS= Number of synonymous substitutions per site, SE: Standard error, Z: Z-test, P: P-value, ndef: non-defective, def: defective.

Table S4 AMOVA with the data published by Kejnovsky et al. (2007) for the *Retand* LTR retrotransposon in the plant *Silene latifolia*. Groups are autosomes, X chromosome and Y chromosome

Source of variation	df	Sum of squares	Variance components	Percentage of variation
Among groups	2	3705.35	20.09	29.98
Within groups	272	12758.23	46.91	70.02
Total	274	16463.58	66.99	

F_{ST}= 0.300

Significance tests (1023 permutations)

Va and F_{ST} : P(rand. value > obs. value) < 0.00001

P(rand. value = obs. value) < 0.00001

P-value < 0.00001±0.00001


4
7
11
1
8
B
X
10
5
6
9
2
3

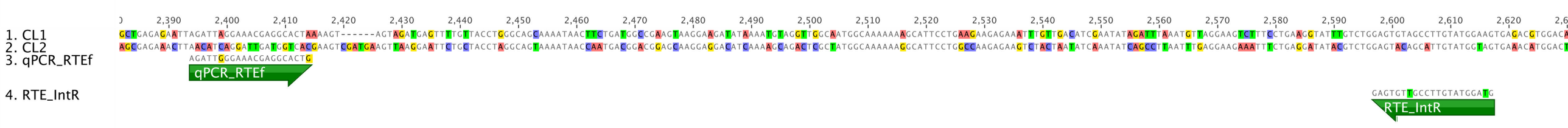
2,390
2,400
2,410
2,420
2,430
2,440
2,450
2,460
2,470
2,480
2,490
2,500
2,510
2,520
2,530
2,540
2,550
2,560
2,570
2,580
2,590
2,600
2,610
2,620
1. CL1
2. CL2
3. qPCR_RTEf
4. RTE_IntR
qPCR_RTEf
RTE_IntR